CSIRO PUBLISHING

Australian Journal of Botany, 2014, **62**, 164–174
http://dx.doi.org/10.1071/BT13209

Genetic diversity and biogeography of the boab *Adansonia gregorii* (Malvaceae: Bombacoideae)

Karen L. Bell[A,B,E], *Haripriya Rangan*[B], *Rachael Fowler*[A,B], *Christian A. Kull*[B], *J. D. Pettigrew*[C], *Claudia E. Vickers*[D] *and Daniel J. Murphy*[A]

[A]Royal Botanic Gardens Melbourne, Birdwood Avenue, South Yarra, Vic. 3141, Australia.
[B]School of Geography and Environmental Science, Monash University, Clayton, Vic. 3800, Australia.
[C]Queensland Brain Institute, University of Queensland, St Lucia, Qld 4072, Australia.
[D]Australian Institute for Bioengineering and Nanotechnology, University of Queensland, St Lucia, Qld 4072, Australia.
[E]Corresponding author. Email: karen.bell@monash.edu

Abstract. The Kimberley region of Western Australia is recognised for its high biodiversity and many endemic species, including the charismatic boab tree, *Adansonia gregorii* F.Muell. (Malvaceae: Bombacoideae). In order to assess the effects of biogeographic barriers on *A. gregorii*, we examined the genetic diversity and population structure of the tree species across its range in the Kimberley and adjacent areas to the east. Genetic variation at six microsatellite loci in 220 individuals from the entire species range was examined. Five weakly divergent populations, separated by west–east and coast–inland divides, were distinguished using spatial principal components analysis. However, the predominant pattern was low geographic structure and high gene flow. Coalescent analysis detected a population bottleneck and significant gene flow across these inferred biogeographic divides. Climate cycles and coastline changes following the last glacial maximum are implicated in decreases in ancient *A. gregorii* population size. Of all the potential gene flow vectors, various macropod species and humans are the most likely.

Additional keywords: Australian monsoon tropics, baobab, dispersal, gene flow, genetic admixture, Kimberley, microsatellite, phylogeography.

Received 23 August 2013, accepted 12 April 2014, published online 22 May 2014

Introduction

The Kimberley region of north-west Australia has high biodiversity and many endemic species. It represents the westernmost region of the Australian monsoon tropics (AMT), characterised by highly seasonal rainfall and savanna vegetation. The Kimberley Plateau is one of the three sandstone blocks in the AMT, along with Arnhem Land and Cape York. It is separated from the neighbouring Arnhem Land Plateau by the lowlands of a former Cretaceous sea floor (Bowman *et al*. 2010). The AMT biome is bounded to the south by arid habitats, which began developing in the Late Cenozoic and contain distinctly different biota (Byrne *et al*. 2008; Bowman *et al*. 2010). Several studies have identified biogeographic barriers between the Kimberley and Arnhem Land plateaus, including the 'Bonaparte Gap', the 'Ord Arid Intrusion', the 'Victoria River Drainage', and the 'Daly River Drainage' (Eldridge *et al*. 2011). Within the Kimberley, a phylogeographic pattern comprising an 'east–west Kimberley divide' (Eldridge *et al*. 2011), has been defined for multiple species (Hill and Johnson 1995; Oliver *et al*. 2010; Melville *et al*. 2011; Potter *et al*. 2012*b*). Heterogeneous environments may have contributed to allopatric divergence through isolation of populations (phylogeographic divergence), and adaptation to different habitat types (ecological divergence). Whereas these studies have provided insights into the distribution and divergence of some endemic Kimberley animal species, there are no similar studies on intraspecific genetic variation of plants. Under the same environmental influences, plant taxa would be expected to exhibit similar patterns of geographic variation to those recorded for animals. This study examines the intraspecific genetic diversity and variation among populations of *Adansonia gregorii* F.Muell. (Malvaceae: Bombacoideae) in the Kimberley. These data are used to test the potential importance of previously identified biogeographic barriers, and their influence on genetic divergence in this species.

Adansonia gregorii (commonly called boab), was first mentioned by Allan Cunningham, naturalist on the HMAS Mermaid, who assigned it to the genus *Capparis*, as *C. gibbosa* (Cunningham 1827). Later, Ferdinand von Mueller, on the Gregory Expedition, recognised the affinity of this taxon with the genus *Adansonia* and named the species *A. gregorii* (von Mueller 1857, 1858). In 2004, the Nomenclature Committee for Spermatophyta ruled to conserve the name *A. gregorii*

(Brummitt 2002), and we use this name in the present paper. *A. gregorii* is an ideal plant taxon for examining geographic variation across the Kimberley, being a significant component of the vegetation and having a distribution that extends across almost the entire Kimberley region and adjacent regions to the east in the Northern Territory (Baum 1995*b*, Baum *et al.* 1998).

Adansonia gregorii is the sole member of the genus *Adansonia* occurring in Australia. Other *Adansonia* species occur in Africa and Madagascar (Baum 1995*b*; Wickens and Lowe 2008; Pettigrew *et al*. 2012). Earlier researchers thought the disjunct distributions of baobabs in Australia, Africa and Madagascar were due to the break-up of Gondwana, although the alternative hypothesis of more recent trans-oceanic dispersal was proposed well before any attempts to date the divergences between species (Raven and Axelrod 1974; Armstrong 1979, 1983). Molecular divergence dating suggests that *A. gregorii* shared a common ancestor with other extant *Adansonia* species in the Miocene, which is too late to be attributable to Gondwanan fragmentation (Baum *et al*. 1998).

Following the Interim Biogeographical Regionalisation for Australia (Australian Government Department of Sustainability 2012), *A. gregorii* is mainly confined to the Dampierland, Central Kimberley, Northern Kimberley and Victoria Bonaparte subregions, with a minor extension eastward into the Ord Victoria Plains (see Fig. 1). To the south, its distribution is bounded by the semiarid environments of the Great Sandy Desert and the Tanami Desert, which are too dry to support the species (Wickens and Lowe 2008). The distribution of *A. gregorii* extends to the coastline which forms the northern bounds of the Kimberley (von Mueller 1893; Gillison 1983; Brock 1988; Baum and Handasyde 1990; Wickens and Lowe 2008). The distributional boundary to the east is less clear. Bowman (1997) questioned why *A. gregorii* is not distributed further east in the Gulf region of the Northern Territory where the environmental conditions are similar to those of north-western Australia. He suggested that its absence might be related to long-term fire history, and that changes in human modification of the landscape in the past two centuries, including overgrazing and changes in fire frequency and

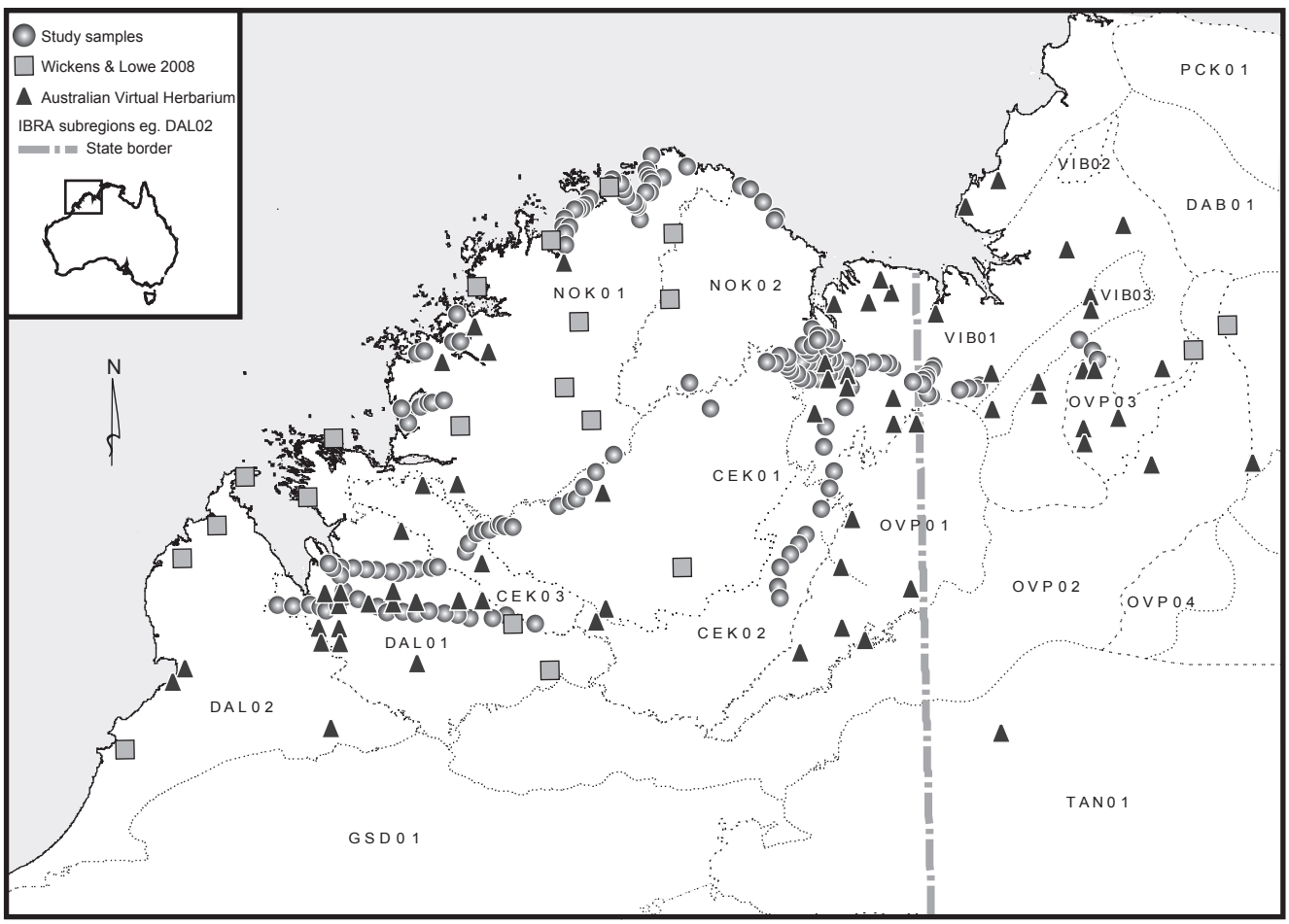

Fig. 1. Recorded distribution of *Adansonia gregorii* taken from the Australian Virtual Herbarium (http://avh.ala.org.au/, accessed 17 April 2014) (triangles) and from Wickens and Lowe (2008) (squares) and localities of samples of *A. gregorii* examined in the present study (circles). Details of these samples are given in Appendix 1 (available as Supplementary Material to this paper). The distribution is overlaid on the subregions of the Interim Biogeographic Regionalisation of Australia (IBRA) (Australian Government Department of Sustainability 2012).

intensity, may be altering the distribution of the species. However, these hypotheses remain untested.

Adansonia gregorii occurs in a wide range of habitats (Wickens and Lowe 2008). The trees are often concentrated along seasonal waterways and flood plains, leading Wickens and Lowe (2008) to suggest that the presence of groundwater is an important factor controlling the species' distribution. However, it does not grow in forests bordering permanent rivers, possibly because of poor competitive ability (Bowman 1997; Wickens and Lowe 2008). The broad habitat range of *A. gregorii* may reflect ecotypes within the species (Beard 1967). The western populations of *A. gregorii* are a significant component of the savanna vegetation in the Fitzroy River Basin. The species also occurs in the more mountainous central Kimberley on drainage lines and in areas with more than 700 mm annual average rainfall. In contrast, in the north and east Kimberley, *A. gregorii* is found on steep shale scarps, and in savanna woodland dominated by *Eucalyptus grandifolia* (Beard 1967).

Materials and methods

Nuclear DNA microsatellite data were generated to investigate the geographic structure of genetic diversity for *A. gregorii*. From these data, statistics of population genetic structure and diversity were calculated, and coalescent analyses were used to estimate divergence times, gene flow between populations, and historical changes in effective population size.

Sampling

Sampling was undertaken over the entire range of *A. gregorii*. Individual trees are often scattered across the landscape, rather than occurring in discrete populations of multiple individuals. Therefore, individuals were not assigned to populations until after analyses of genetic structure were completed. We sampled 220 individuals from different, broadly distributed locations throughout the species' known distribution in Australia (Fig. 1). Leaf material was dried and preserved with silica gel. Herbarium specimens were collected for a subset of the samples, and deposited in the National Herbarium of Victoria (MEL) and the Northern Territory Herbarium (DNA). For details see Appendixes 1 and 2, available as Supplementary Material to this paper.

DNA isolation, cpDNA sequencing and microsatellite genotyping

Genomic DNA was extracted from dried leaf material using the DNeasy Plant Mini Kit (Qiagen, Valencia, CA, USA), following the manufacturer's instructions with modifications as described in Pettigrew *et al*. (2012). For a subset of 10–20 individuals selected from across the range of the species (see Appendix 3 for details), we amplified three chloroplast DNA (cpDNA) spacer regions, *trn*C–*ycf*6, *ndh*F–*rpL*32, and *3′trn*V–*ndh*C, using the primers of Shaw *et al*. (2007). These were selected because they had previously been found to be variable in *Adansonia* species (K. L. Bell & D. J. Murphy, unpubl. data). The PCR cycling conditions were: 95°C 15 min; (95°C 1 min, 50°C 1 min, 72°C 4 min) × 30 cycles; 72°C 5 min. Following amplification, PCR products were sequenced by Macrogen (Seoul, Korea) using Big-Dye terminator chemistry (Applied Biosystems, Foster City, CA, USA), and read on a 3730 sequencer (Applied Biosystems). Trace files were imported into Geneious (Biomatters, Auckland, New Zealand), trimmed, and forward and reverse sequences assembled into consensus sequences.

Microsatellites were used for population genetic analysis. Primers for 18 microsatellite loci were initially developed for *A. digitata*, and 12 of the 18 were found to amplify in *A. gregorii* (Larsen *et al*. 2009). We screened these 12 loci in a subset of seven *A. gregorii* samples and selected six loci (Ad06, Ad08, Ad13, Ad14, Ad15, and Ad18) that were found to be routinely amplifiable and polymorphic in *A. gregorii*. Amplified loci were sequenced to test for homology with the microsatellites amplified in *A. digitata.* Forward primers for the six microsatellite loci were appended with a 454A adaptor sequence, following the method of James *et al*. (2011). Microsatellite amplification reactions comprised: 1× Type-It Multiplex PCR Master Mix (Qiagen), 0.075 µM of the forward primer, 0.25 µM of the reverse primer, 0.2 µM of the 454A primer fluorescently labelled with 6-FAM, Vic., NED or PET fluorescent dyes (Applied Biosystems), and 2.0 µL of template DNA in a total volume of 10 µL. The PCR cycling conditions were as described in the Type-It Microsatellite PCR Kit instruction manual, with an annealing temperature of 60°C for all loci except Ad15, for which an annealing temperature of 54°C was used. Amplified PCR product was checked for quality on a 1.5% agarose gel. Following PCR amplification, individual loci with different fluorescent dyes were multiplexed in equal concentrations and run by Macrogen on a 3730XL sequencer (Applied Biosystems), with a GS500 LIZ size standard. Data were visualised and allele sizes scored in Peak Scanner (Applied Biosystems). We tested the six loci for deviations from Hardy–Weinberg equilibrium using GENALEX version 6.41 (Peakall and Smouse 2006).

Geographic structure

A priori population delimitation within *A. gregorii* was not assumed but tested with different methods. Geographic structure of genetic diversity was investigated using a Bayesian probabilistic approach implemented in STRUCTURE version 2.3.3 (Pritchard *et al*. 2000). An admixture model, with correlated gene frequencies (Falush *et al*. 2003), was used to calculate the likelihood of different values for the number of populations (K). Simulations consisted of a burn-in of 50 000 iterations followed by 100 000 Markov chain Monte Carlo (MCMC) iterations. Ten runs for each of $K = 1–10$ were carried out on an SGI Altix XE Cluster through the Victorian Life Sciences Computing Initiative. The value(s) of K that best explained the structure in the data was determined using STRUCTURE HARVESTER WEB version 0.6.93 (Earl and von Holdt 2012), following the ΔK method of Evanno *et al*. (2005). Multiple runs at the appropriate value(s) of K were combined using CLUMPP version 1.1.2 (Jakobsson and Rosenberg 2007), and plotted graphically using DISTRUCT version 1.1 (Rosenberg 2004).

The microsatellite data was further analysed using TESS version 2.3.1, because the incorporation of geographic data

makes this approach more sensitive than STRUCTURE analysis in detecting clusters under subtle geographic structure (François *et al*. 2006; Chen *et al*. 2007). Like STRUCTURE, TESS uses a Bayesian probabilistic approach to recognise genetic clusters but, unlike STRUCTURE, it comprises a simultaneous analysis of multilocus genotypes and geographic data. A BYM admixture model was used to calculate the likelihood under different values for K_{max} (2–10). Simulations consisted of a burn-in of 50 000 iterations followed by 100 000 iterations of sampling. The value(s) of K that best explained the structure in the data was determined by plotting the deviance information criterion against K_{max} to find the point where the deviance information criterion stabilised. Multiple runs at the appropriate value(s) of K_{max} were combined using CLUMPP version 1.1.2 (Jakobsson and Rosenberg 2007), and plotted graphically using DISTRUCT version 1.1 (Rosenberg 2004).

Genetic structure was also tested using a spatial principal components analysis (sPCA). This method was preferred over a PCA due to its treatment of spatial autocorrelation (Moran's *I*) in conjunction with genetic data (Jombart *et al*. 2008; Balzarini *et al*. 2011). The analysis was conducted using the 'adegenet' package (Jombart *et al*. 2008) for R software (R Development Core Team 2008). Following preliminary analyses testing various connection network methods, a neighbourhood by distance connection network (0–100 km) was used to link localities. The significance of global and local patterns of genetic diversity (significant positive and negative correlations with Moran's *I*, respectively), against random spatial distribution of genetic variance was assessed with a Monte Carlo-based test (9999 iterations), as described in Jombart *et al*. (2008). The first two PC were mapped in geographic space, and examined visually to cluster samples into genetically and geographically distinct populations. Statistical support for these populations was assessed with analysis of molecular variance (AMOVA; Excoffier *et al*. 1992) in GENALEX version 6.41 (Peakall and Smouse 2006). Analyses were based on the Φ_{PT} measure of genetic diversity, with 999 permutations.

Isolation by distance (IBD) was examined through a Mantel test (linear codominant genetic distance versus [ln (1 + geographic distance)]; 999 permutations) conducted in GENALEX version 6.41 (Peakall and Smouse 2006). Since geographic structure due to genetic clustering and due to IBD can be confounded, further tests were conducted to separate these effects (Meirmans 2012). To remove the confounding effect of genetic clustering when inferring IBD, a Mantel test was carried out with random permutations only within populations. Conversely, to eliminate the confounding effect of IBD when inferring genetic clusters, a partial Mantel test of genetic distance versus population (0 for samples from the same population, 1 for samples from different populations) was conducted with geographic distance as a covariate.

Genetic diversity

Genetic diversity statistics were calculated for the entire range of *A. gregorii*, and within each population as defined by sPCA. GENALEX version 6.41 (Peakall and Smouse 2006) was used to calculate the number of alleles per locus, effective number of alleles per locus, number of private alleles per locus, Shannon's information index, observed heterozygosity, expected heterozygosity under Hardy–Weinberg equilibrium, and fixation index F (inbreeding coefficient). GENALEX was also used to calculate F_{ST} between populations and across the entire range, based on 999 random permutations of the data.

A lack of cpDNA variation suggested that *A. gregorii* populations may have experienced a genetic bottleneck. Therefore, deviations from mutation-drift equilibrium were tested using BOTTLENECK version 1.2.02 (Cornuet and Luikart 1996) to determine whether recent changes in effective population size had occurred. Expected heterozygosities under mutation-drift equilibrium were simulated with 1000 replications under the two-phased model of mutation (TPM) with default settings (variance 30, 70% of mutations fitting the stepwise mutation model). Three statistical tests are available in the BOTTLENECK software to compare observed versus expected heterozygosities. The 'standardised differences test' is unsuitable for less than 20 loci (Cornuet and Luikart 1996). We therefore used the 'sign test' and 'Wilcoxon sign-rank test', which are less sensitive to the low number of loci, and the allele frequency distribution was compared with that expected under the null model (Luikart *et al*. 1998).

Coalescent modelling

Population parameters associated with divergence between pairs of populations detected based on other analyses were estimated using IMA2 (Hey and Nielsen 2004). This method analyses genotypes of individuals within populations via a coalescent model to estimate divergence time ($t = \mathbf{tu}$, where **t** is absolute time and **u** is the neutral mutation rate), migration rate between populations ($m = \mathbf{m}/\mathbf{u}$, where **m** is the rate of migration for each gene copy), and population sizes for extant and ancestral populations ($\theta = 4\mathbf{Nu}$, where **N** is the effective population size of a population of diploid individuals). We used a stepwise mutation model of molecular evolution for each of the microsatellite loci (the TPM model used for the BOTTLENECK analysis is unavailable in IMA2). Four MCMC analyses with independent random starting points were run for each population comparison. Each MCMC analysis consisted of 100 heated chains under a geometric heating scheme with heating parameters ranging from 0.3 to 0.995. The MCMC chains were initially run in 'IMburn-in' mode, with plots of likelihood values recorded every 4 h. Once likelihood values had stabilised in all four independent runs, chains were switched to 'IMrun' mode, with sampling every 100 steps. Convergence on stationary distributions of parameters was assessed based on the similarity of posterior distributions of independent runs, and analyses were stopped when convergence was achieved. For each divergence, the saved MCMC runs from all four analyses were combined, and coalescent parameters were estimated as the mode of the posterior probability distribution, with a credibility interval corresponding to the 95% highest posterior density. Likelihood ratio tests were used to test different divergence scenarios, with two times the log-likelihood ratio expected to follow a chi-square distribution. Specifically, we assessed whether migration rates were significantly asymmetrical or significantly greater than zero,

and whether effective population sizes in extant and ancestral populations were significantly different.

For purposes of comparison, MIGRATE-N (Beerli 2009) was also used to estimate m and θ. A stepwise mutation model of molecular evolution was applied to each of the microsatellite loci, allowing variation of mutation rates among loci. Analyses were run on an SGI Altix XE Cluster through the Victorian Life Sciences Computing Initiative. Two parallel Bayesian MCMC analyses (Beerli and Felsenstein 2001; Beerli 2006) with independent random starting points were run for each hypothesised divergence. Each MCMC analysis consisted of 16 heated chains with heating parameters of 1.00, 1.17, 1.40, 1.75, 2.33, 3.50, 7.00, and 1 000 000.00. Starting points for genealogies and demographic parameters were based on the UPGMA tree and F_{ST}. Bayesian uniform priors for θ and m were bound between 0 and 50, and between 0 and 100, respectively. A burn-in of 100 000 steps for each locus was discarded. Following burn-in, the chains were run with sampling every 10 steps, for a further 50 000 recorded steps for each locus. Convergence of parameters was assessed based on the similarity of posterior distributions of independent runs, and the effective sample size.

Relative divergence times, population sizes, and rates of gene flow were converted to absolute values, following both methods of coalescent analysis, using a generation time of 20 years, the generally accepted age of first flowering (Wickens and Lowe 2008), and estimated mutation rates of 2.4×10^{-4} mutations per generation (based on direct observation of microsatellite mutation rate in wheat; Thuillet *et al*. 2002) and 5.0×10^{-4} mutations per generation (considered to be the average mutation rate over many species; Estoup *et al*. 2002; Sun *et al*. 2009).

Results

cpDNA sequencing

For each chloroplast region, the majority of individuals shared the same common haplotype (for details, see Appendix 3, available as Supplementary Material to this paper). For *trn*C–*ycf*6, two haplotypes were detected, with one of these present in a single individual. For *ndh*F–*rpL*32 and for *3′trn*V–*ndh*C, three haplotypes were detected, with two only present in single individuals. Since all variation occurred as private alleles, this information was uninformative for phylogeographic analysis. Hence, we relied on microsatellite data to assess genetic structure.

Microsatellite data

Flanking regions and microsatellite motifs in *A. gregorii* matched those of *A. digitata* (Larsen *et al*. 2009) for all loci

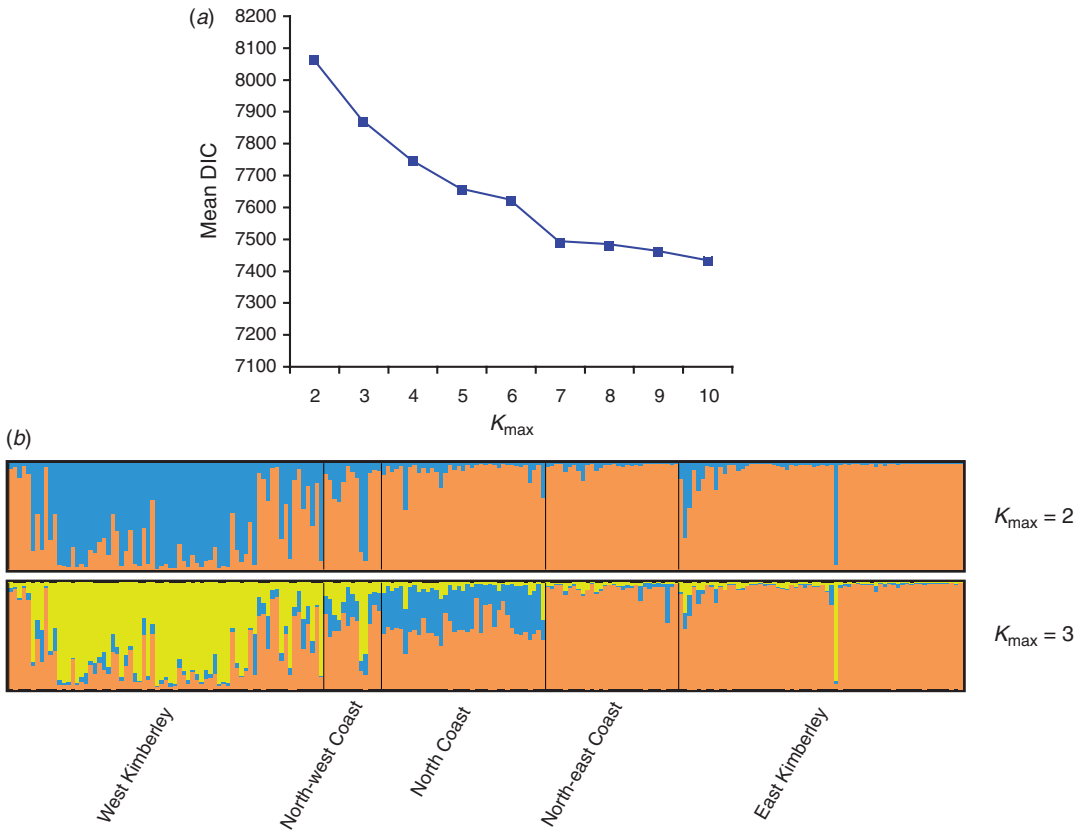

Fig. 2. Bayesian probabilistic analysis of multilocus genotypes of *Adansonia gregorii* and geographic data using a BYM admixture model in TESS version 2.3.1 under different values for K_{max} (2–10). (*a*) Plot of deviance information criterion against K_{max}. (*b*) Admixture proportion of individuals in genetic clusters at $K_{max} = 2$ and $K_{max} = 3$, following combination of multiple TESS runs using CLUMPP version 1.1.2.

with the exception of Ad18, which had a different motif. Rather than the TG microsatellite repeat recorded for Ad18 in *A. digitata*, an AT microsatellite repeat in an adjacent position was found in *A. gregorii*. Only one locus (Ad06) was found to deviate from Hardy–Weinberg equilibrium for multiple populations (Appendix 4, available as Supplementary Material to this paper), so we considered our dataset to be suitable for subsequent analyses.

Geographic structure

Bayesian analysis using STRUCTURE gave a maximum mean likelihood at $K = 1$, with high likelihoods for $K = 2$ and 3, dropping substantially from $K = 4$ onwards (Appendix 5, available as Supplementary Material to this paper). The maximum value for the ΔK statistic, representing the value of K that best explains the structure in the data (Evanno *et al*. 2005), occurred at $K = 3$ (Appendix 5). However, the ΔK statistic is unable to infer a K of <2, and at $K = 2$ and $K = 3$ all individuals showed admixture between clusters (Appendix 5). This suggests that $K = 1$ may provide a better explanation of the structure, or lack thereof, in the data.

TESS did not give a clear indication of the number of populations: the probabilities gradually decreased with increasing K_{max}, rather than suddenly dropping after the appropriate value of K (Fig. 2*a*). This would be consistent with $K = 1$. However, in contrast to the STRUCTURE analysis, TESS was able to assign individuals to populations at $K = 2$ (Fig. 2*b*), with some differentiation between the west and the east of the species range. At $K = 3$, the pattern was less clear, with many individuals showing admixture between clusters (Fig. 2*c*).

The sPCA analysis inferred significant geographic structure. The first PC had significant global structure (i.e. positive correlation with Moran's I; $P = 0.0001$) whereas the second PC had weaker structure ($P = 0.0032$). For each sample, the scores of the first two principal components were plotted on a distribution map (Fig. 3*a*, *b*). The first PC divided samples quite sharply into west and east groups. The second PC divided the west group into three clusters, West Kimberley (WK), North-west Coast (NWC), and North Coast (NC), and the east group into two clusters, North-east Coast (NEC) and East Kimberley (EK) (Fig. 3*a*, *b*). We treated these five clusters as operational populations for subsequent analyses.

The validity of the population structure was tested using AMOVA. A two-level AMOVA estimated that genetic variation among west and east regions and among populations was partitioned with 1% among regions, 3% among populations within regions, and 96% within populations. Despite low levels of genetic variation between populations, divergence among populations within regions and across the entire range was significantly higher than expected by chance ($\Phi_{PR} = 0.028$; $P = 0.001$ and $\Phi_{PT} = 0.038$; $P = 0.001$). Pairwise F_{ST} was significant for most population pairs (Table 1), the exceptions being NC–NWC and NEC–EK. A Mantel test for IBD was significant across the entire range ($r = 0.057$; $P = 0.009$). However, additional Mantel tests and partial Mantel tests were unable to separate the confounding effects of potential biogeographic barriers and IBD. The test with permutations only within the five

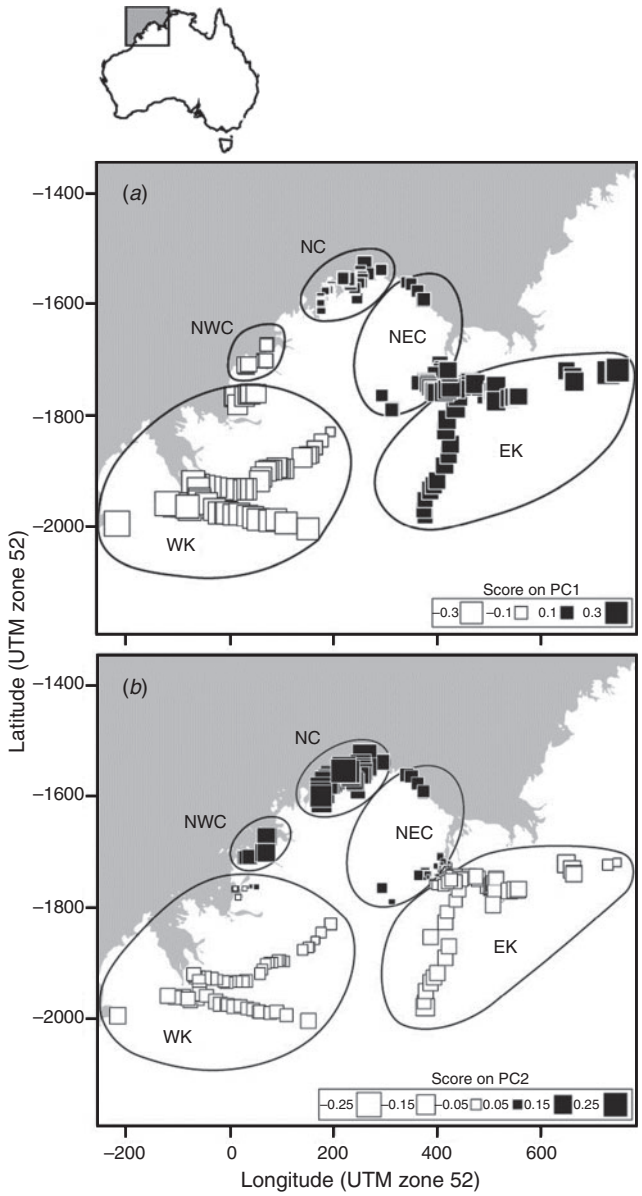

Fig. 3. Five inferred populations of *Adansonia gregorii* as determined by spatial principal components analysis (sPCA). (*a*) The first PC (significant global structure, i.e. positive correlation with Moran's I, $P = 0.0001$), demonstrating differentiation between samples in the east and west of the species range. (*b*) The second PC (significant global structure, $P = 0.0032$), which distinguishes between coastal and inland samples. On the basis of visual examination of the sPCA, the samples are divided into: WK = West Kimberley; NWC = North-west Coast; NC = North Coast; NEC = North-east Coast; EK = East Kimberley.

populations was not significant ($r = 0.066$; $P = 0.267$), suggesting that IBD is not occurring within populations, and that geographic structure is more likely a result of population clustering. However, the test for population clustering with geographic distance as a covariate was also non-significant ($r = 0.007$; $P = 0.285$), which would suggest that variation is due to IBD (Meirmans 2012). In combination, these tests demonstrate that genetic differentiation within

A. gregorii can be explained by simple IBD without a need to invoke particular biogeographic barriers to gene flow.

Genetic diversity statistics

Observed heterozygosity in *A. gregorii* varied from 0.58 in NEC, to 0.68 in WK, and was 0.63 across the entire species range. Expected heterozygosity varied from 0.61 in NWC, NEC and EK, to 0.68 in WK, and was 0.65 across the entire species range (Table 2, Appendix 6, available as Supplementary Material to this paper). We found no evidence of inbreeding in *A. gregorii* ($F = 0.02$; Table 2). Tests for deviations from mutation-drift equilibrium, based on the 'sign test' and 'Wilcoxon test' in BOTTLENECK were unable to detect any recent reductions in effective population size. However, this does not rule out older bottlenecks, more than a few hundred generations in the past (Cornuet and Luikart 1996).

Coalescent modelling

Coalescent modelling was used to look at the population clusters defined by sPCA. We modelled west (WK, NWC) to east (NC, NEC, EK) and coast (NWC, NC, NEC) to inland (WK, EK) groupings. Burn-in was achieved after 218 216 iterations for the west–east divergence, and after 474 472 iterations for the coast–inland divergence, while convergence occurred after 807 808 and 2 526 525 iterations, respectively. As summarised in Tables 3 and 4, IMA2 inferred divergence times (t) with credibility intervals including zero for both the west–east and coast–inland groupings. This result suggests only minimal divergence and high levels of gene flow. However, although significant gene flow was inferred in all directions, the estimated migration rate from west to east was higher than in the opposite direction (Tables 3, 4). In contrast, analysis of coast and inland samples did not detect a statistically significant asymmetry in migration (Tables 3, 4). Estimates of effective population sizes (θ) of extant populations using both IMA2 and MIGRATE-N yielded similar results with reasonably narrow confidence intervals (Table 3). The ancestral θ for the east–west divergence was significantly higher than the extant population estimate for the east. The coast–inland divergence was also associated with a statistically significant change in θ, with θ of both extant populations smaller than the ancestral θ. The results demonstrate a historical population bottleneck for *A. gregorii.* This is in contrast to the results of the BOTTLENECK analysis and is likely to reflect older population size changes that could not be detected through comparisons of expected and observed heterozygosity.

Table 1. Population differentiation (F_{ST}) in *Adansonia gregorii*
Statistical significance was determined with 999 permutations: n.s. $P \geq 0.05$; *$P < 0.05$; **$P < 0.01$; ***$P < 0.001$. Populations are as defined in Fig. 3

	West Kimberley (WK)	North-west Coast (NWC)	North Coast (NC)	North-east Coast (NEC)	East Kimberley (EK)
WK	–	–	–	–	–
NWC	0.015***	–	–	–	–
NC	0.016*	0.006n.s.	–	–	–
NEC	0.025***	0.003n.s.	0.012n.s	–	–
EK	0.014**	0.006n.s	0.027*	0.002n.s.	–

Discussion

Spatial genetic structure

Spatial genetic structure across the range of *A. gregorii* is limited, with most analyses inferring that a single, panmictic population is most likely. Only analyses incorporating geographic data as a covariate (TESS and sPCA) were able to detect geographic structure, specifically differentiation between west (NWC, WK populations) and east (EK, NEC, NC populations) and between coastal (NWC, NC, NEC) and inland (WEK, EK) populations. The former is broadly congruent with the previously identified east–west Kimberley divide (Eldridge *et al.* 2011; Potter *et al.* 2012*b*), extending from the north-western coast around the mouth of the Prince Regent River and across the Central Kimberley toward the south-western Kimberley ranges (Fig. 4). The latter divide extends from the Macdonald Range in the north-west across the Gardner Plateau to the Cambridge Gulf. It is worth noting that the east–west divide broadly coincides with differences between the *A. gregorii* ecotypes suggested by Beard (1967).

Gene flow

The lack of geographic structure is most easily explained by strong gene flow across the *A. gregorii* range. This suggests

Table 2. Genetic diversity statistics (mean ± s.d.) of *Adansonia gregorii* for each population, and across the entire range
n = number of samples; N_a = number of alleles per locus; N_e = effective number of alleles per locus; I = Shannon's Information Index; H_o = observed heterozygosity; H_e = expected heterozygosity under Hardy–Weinberg equilibrium; UH_e = unbiased expected heterozygosity = $[2N/(2N - 1)] * H_e$; F = Wright's allelic fixation index. Geographic ranges of the populations are outlined in Fig. 3. Statistics for individual loci are reported in Appendix 6, available as Supplementary Material to this paper

	West Kimberley (WK)	North-west Coast (NWC)	North Coast (NC)	North-east Coast (NEC)	East Kimberley (EK)	Entire range
n	69.83 ± 0.40	13.00 ± 0.00	36.83 ± 0.17	30.00 ± 0.00	62.83 ± 0.60	212.50 ± 0.88
N_a	11.83 ± 3.23	6.17 ± 1.70	8.00 ± 2.46	7.67 ± 2.16	8.33 ± 2.43	13.50 ± 3.98
N_e	5.33 ± 2.08	3.20 ± 0.75	4.31 ± 1.61	3.32 ± 0.77	3.48 ± 0.95	4.63 ± 1.78
Private alleles	2.00 ± 2.28	0.17 ± 0.41	0.33 ± 0.52	0.17 ± 0.41	0.17 ± 0.41	n.a.
I	1.65 ± 0.35	1.27 ± 0.26	1.41 ± 0.32	1.31 ± 0.27	1.32 ± 0.28	1.57 ± 0.35
H_o	0.68 ± 0.06	0.59 ± 0.09	0.63 ± 0.08	0.58 ± 0.09	0.59 ± 0.07	0.63 ± 0.07
H_e	0.68 ± 0.08	0.61 ± 0.08	0.64 ± 0.08	0.61 ± 0.09	0.61 ± 0.09	0.65 ± 0.09
UH_e	0.69 ± 0.09	0.63 ± 0.08	0.65 ± 0.08	0.62 ± 0.09	0.61 ± 0.09	0.66 ± 0.09
F	–0.040 ± 0.067	0.024 ± 0.079	0.019 ± 0.030	0.029 ± 0.076	–0.003 ± 0.076	0.02 ± 0.05

high propagule dispersal ability of the species, and possibly expansion from a recent introduction or small refugial population. Several dispersal vectors have been previously proposed for species of *Adansonia* (Wickens and Lowe 2008; and references therein). Gene flow of the paternal line may occur through pollination, with various birds, hawkmoths, and possibly other insects and bats recorded as pollinators (Baum and Handasyde 1990; Baum 1995*a*; Bowman 1997; Lowe 1998; Wickens and Lowe 2008; G. Rethus and J. D. Pettigrew, unpubl. data). However, gene flow involving the entire genome would require dispersal of seeds. Floodwaters could be a long-distance dispersal mechanism in *Adansonia* species (Wickens 1982; Baum 1995*b*), but in the case of *A. gregorii*, such a mechanism may be limited to the edges of seasonal waterways and alluvial flats, owing to the fragile and dehiscent nature of its pod (Baum 1995*b*; Bowman 1997). The most likely long-distance dispersal agents of boab fruits and seeds would be mammals, including humans (Bowman 1997). Rock wallabies (*Petrogale* spp.), wallabies and kangaroos (*Macropus* spp.) eat the fruit and disperse the seeds in their scats (Wickens and Lowe 2008). However, the phylogeography of the short-eared rock-wallaby (*P. brachyotis*), one of the more vagile rock-wallaby species in the Kimberley (Potter *et al*. 2012*a*), showed a strong east–west divergence (Potter *et al*. 2012*b*), much stronger than is seen in *A. gregorii*. Among the other potential dispersal agents, humans might have played an important role in boab gene flow over

Table 3. Absolute values of divergence and gene flow parameters among populations of *Adansonia gregorii* estimated using coalescent analyses

For each parameter, the mode of the posterior probability density is presented, with the range containing 95% of the posterior probability density in parentheses. For the east–west divergence, 0 refers to the western samples (WK and NWC) and 1 refers to the eastern samples (NC, NEC and EK). For the coastal–inland divergence, 0 refers to the coastal samples (NWC, NC and NEC) and 1 refers to the inland samples (WK and EK). The parameters for each divergence event are presented in two rows. The top row of numbers has been converted to absolute values assuming a neutral mutation rate of 5.0×10^{-4} mutations per generation, while the bottom row assumes a rate of 2.4×10^{-4}. Parameters are abbreviated as follows: t is divergence time; N_i is the effective population size of population i; N_A is the ancestral effective population size; $m_{i \rightarrow j}$ is the rate of migration from population i to population j. Migration rates are presented in real time, i.e. from past to present. Geographic ranges of the populations are outlined in Fig. 3

Divergence	Analysis method	t (years)	N_0 (effective population size)	N_1 (effective population size)	N_A (effective population size)	$m_{0 \rightarrow 1}$ (individuals per year)	$m_{1 \rightarrow 0}$ (individuals per year)
West–east	IMA2	3600 (0–10 800)	2050 (750–4050)	1550 (750–5250)	5850 (4150–9550)	0.47 (0.05–3.64)	0.11 (0.008–7.94)
	–	7690 (0–23 100)	4380 (1600–8650)	3310 (1600–11 200)	12500 (8870–20 400)	0.47 (0.05–3.64)	0.11 (0.008–7.94)
	Migrate-n	n.a.	1780 (1120–2380)	1680 (970–3400)	n.a.	2.76 (0.81–7.04)	1.11 (0.39–2.10)
	–	n.a.	3700 (2330–4970)	3490 (2010–7080)	n.a.	2.76 (0.81–7.04)	1.11 (0.39–2.10)
Coast–inland	IMA2	400 (0–7600)	250 (150–1950)	550 (250–3850)	5450 (3650–8250)	0.74 (0.08–21.58)	0.51 (0.03–11.72)
	–	855 (0–16 200)	534 (321–4170)	1180 (534–8230)	11 600 (7800–17 600)	0.74 (0.08–21.58)	0.51 (0.03–11.72)
	Migrate-n	n.a.	942 (317–1600)	2010 (677–3420)	n.a.	1.62 (0.91–2.42)	0.07 (0.005–0.21)
	–	n.a.	2010 (677–3420)	5470 (3560–7230)	n.a.	1.62 (0.91–2.42)	0.07 (0.005–0.21)

Table 4. Likelihood ratio tests for significance of migration rates and directions based on IMA2 analyses of divergences among *Adansonia gregorii* populations

Higher log-likelihood ratios indicate that the restricted model under examination is less likely than the full model allowing unrestricted migration in all directions and unrestricted effective population sizes. Where the likelihood of the restricted model is significantly less than the full model ($P \leq 0.05$), this is indicated with an asterisk

Divergence	Migration model	log(P)	Number of terms	Degrees of freedom	2 log-likelihood ratio
East–west	Full model (all migration rates and population sizes free to vary)	–4.01	5	–	–
	Migration rates equal	–4.494	4	1	0.9679
	No migration from east to west	–28.8	4	1	49.57*
	No migration from west to east	–41.1	4	1	74.17*
	No migration	–509.6	3	2	1011*
	East and west population sizes equal	–4.187	4	1	0.3523
	West and ancestral population sizes equal	–5.182	4	1	2.342
	East and ancestral population sizes equal	–6.907	4	1	5.792*
	All population sizes equal	–15.77	3	2	23.52*
Coast–inland	Full model (all migration rates and population sizes free to vary)	–4.62	5	–	–
	Migration rates equal	–5.642	4	1	2.044
	No migration from inland to coast	–507.9	4	1	1007*
	No migration from coast to inland	–905.1	4	1	1801*
	No migration	–3824	3	2	7638*
	Coast and inland population sizes equal	–5.917	4	1	2.594
	Coast and ancestral population sizes equal	–44.19	4	1	79.15*
	Inland and ancestral population sizes equal	–7.025	4	1	4.809*
	All population sizes equal	–46.11	3	2	82.98*

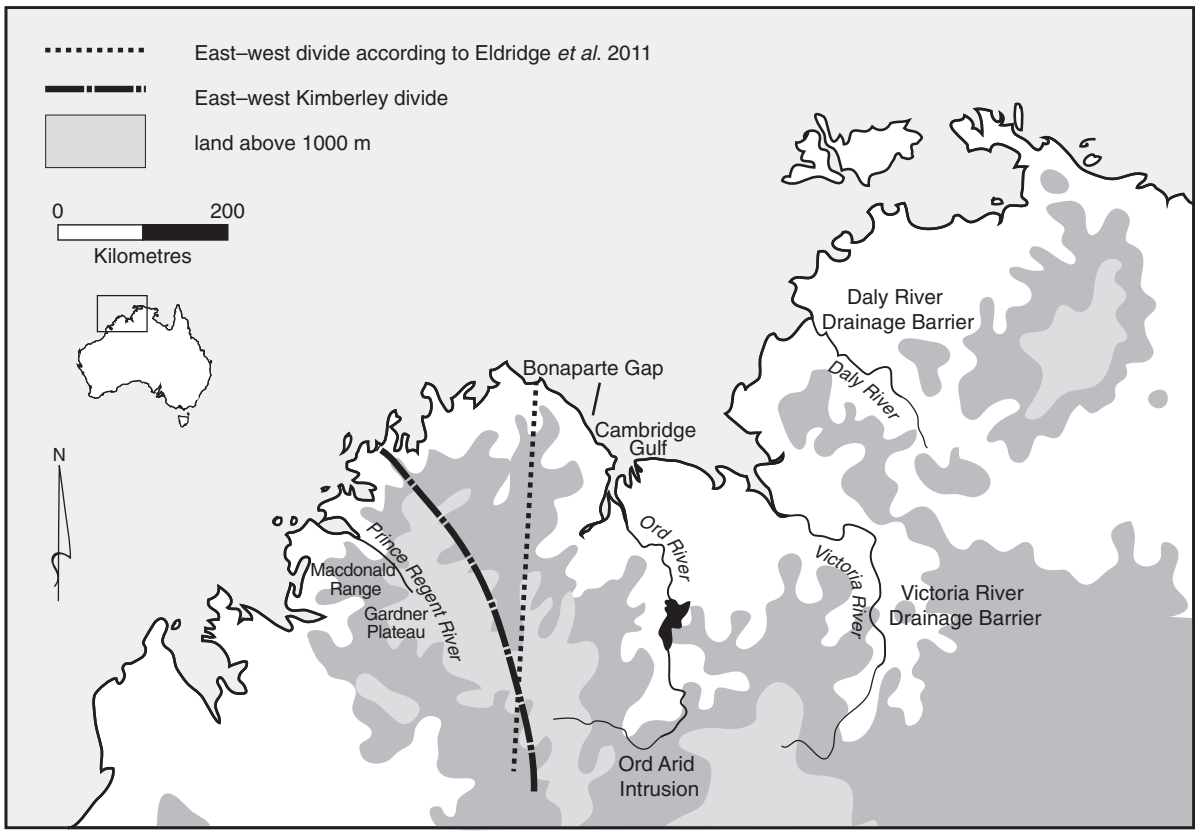

Fig. 4. Localities of four putative biogeographic barriers across north-western Australia, the 'Bonaparte Gap', the 'Ord Arid Intrusion', the 'Victoria River Drainage', and the 'Daly River Drainage', which together form the 'Kimberley Plateau–Arnhem Land Barrier', with a further barrier defined within the Kimberley, the 'east–west Kimberley divide', modified from Eldridge *et al.* (2011). The most striking divergence for *A. gregorii* populations is between west (NWC, WK) and east (EK, NEC, NC). This additional barrier is represented by a dashed line on the map.

the past several thousand years. Boabs have been found near aboriginal middens in western Kimberley (Boland *et al.* 1985), and there is archaeobotanical evidence of consumption of boab fruit by Aboriginal groups over millennia in the Kimberley (McConnell and O'Connor 1997,1999; Wallis 2001). The prehistoric rock art in the northern Kimberley also reflects possible representations of the tree, indicating its cultural significance to ancient human groups that may have occupied this region (Pettigrew 2011). Thus, as has been found for the African baobab (Duvall 2007; Assogbadjo *et al.* 2010), it seems likely that humans transporting the fruit as a food source have significantly shaped the current distribution of genetic variation in *A. gregorii*.

Genetic diversity and effective population size

We detected low genetic diversity in cpDNA, but moderate diversity in microsatellites of *A. gregorii*. We were unable to detect recent changes in effective population size via tests for deviation from mutation-drift equilibrium (BOTTLENECK), but detected older population size changes using coalescent analyses (IMA2 and MIGRATE-N). This older population bottleneck may correspond to unfavourable climates and rising sea levels following the last glacial maximum 26.5–19 ka (Clark *et al.* 2009). During the Last Glacial Maximum the continental shelf extended far beyond the present coastline (Kershaw 1995). Rising sea levels from 17 to 8 ka would have flooded this previously exposed continental shelf where boabs were likely to have been abundant (Kershaw 1995). These changes would have reduced the overall boab population size and set the stage for dispersal inland, as demonstrated by patterns of inferred gene flow.

Conclusions

The main findings of the present study are a lack of strong genetic structure in *A. gregorii*, suggestive of high levels of gene flow, and some evidence of an ancient genetic bottleneck. This pattern is most easily explained as being a result of efficient gene flow, perhaps mediated in part by humans, along with climatic fluctuations and changing coastlines at the end of the last glacial cycle. Future studies using information from other sources such as archaeology, linguistics or palaeo-anthropology may improve our understanding of the migration patterns and distributions of prehistoric social groups in the Kimberley and their potential role in the dispersal and distribution of *A. gregorii.*

Acknowledgements

This project was funded through ARC discovery project DP1093100 (H. Rangan, D. J. Murphy and C. A. Kull). This research was supported by a Victorian Life Sciences Computation Initiative grant number VR0165 on its Peak Computing Facility at the University of Melbourne, an initiative of the

Victorian Government, Australia. We thank the following people and organisations: Kara Rasmanis for producing the figures; David Baum (University of Wisconsin-Madison), Joanne Birch, Elizabeth James, Mark McDonnell (Royal Botanic Gardens Melbourne) and four anonymous reviewers for advice on analysis and comments on the manuscript; the DEC (WA) and DNREAS (NT) for providing permits for field work. Author contributions: H. R., C. A. K. and D. J. M. initiated the research project, framed the objectives and provided research facilities; J. D. P., K. L. B. and H. R. collected the samples; K. L. B., R. F. and C. E. V. carried out laboratory procedures; K. L. B. and R. F. analysed the data; K. L. B. and H. R. wrote the paper with contributions from all other authors.

References

Armstrong P (1979) The history, natural history and distribution of *Adansonia*: a plant genus of the Indian Ocean littoral. In 'The Indian Ocean in focus. International conference on Indian Ocean studies, Perth, Western Australia 1979. Section I. Environment and resources'. (Ed. P Reeves) pp. 1–21. (Perth Building Society: Perth)

Armstrong P (1983) The disjunct distribution of the genus *Adansonia* L. *The National Geographical Journal of India* **29**, 142–163.

Assogbadjo AE, Glele Kakai R, Kyndt T, Sinsin B (2010) Conservation genetics of baobab (*Adansonia digitata* L.) in the parklands agroforestry systems of Benin (West Africa). *Notulae Botanicae Horti Agrobotanici Cluj-Napoca* **38**, 136–140.

Australian Government Department of Sustainability, Environment, Water, Population and Communities (2012) 'IBRA version 7.' (Canberra)

Balzarini M, Teich I, Bruno C, Peña A (2011) Making genetic biodiversity measurable: a review of statistical multivariate methods to study variability at gene level. *Revista de la Facultad de Ciencias Agrarias* **43**, 261–275.

Baum DA (1995*a*) The comparative pollination and floral biology of baobabs (*Adansonia* – Bombacaceae). *Annals of the Missouri Botanical Garden* **82**, 322–348. doi:10.2307/2399883

Baum DA (1995*b*) A systematic revision of *Adansonia* (Bombacaceae). *Annals of the Missouri Botanical Garden* **82**, 440–471. doi:10.2307/2399893

Baum DA, Handasyde T (1990) The boab tree (*Adansonia gregorii*) in north-west Australia. Unpublished report in Western Australian Herbarium Library, Perth.

Baum DA, Small RL, Wendel JF (1998) Biogeography and floral evolution of baobabs (*Adansonia*, Bombacaceae) as inferred from multiple data sets. *Systematic Biology* **47**, 181–207. doi:10.1080/106351598260879

Beard JS (1967) Some vegetation types of tropical Australia in relation to those of Africa and America. *Journal of Ecology* **55**, 271–290. doi:10.2307/2257877

Beerli P (2006) Comparison of Bayesian and maximum likelihood inference of population genetic parameters. *Bioinformatics* **22**, 341–345. doi:10.1093/bioinformatics/bti803

Beerli P (2009) How to use migrate or why are markov chain monte carlo programs difficult to use? In 'Population genetics for animal conservation'. (Eds G Bertorelle, MW Bruford, HC Hauffe, A Rizzoli, C Vernesi) pp. 42–79. (Cambridge University Press: Cambridge, UK)

Beerli P, Felsenstein J (2001) Maximum likelihood estimation of a migration matrix and effective population sizes in n subpopulations by using a coalescent approach. *Proceedings of the National Academy of Sciences, USA* **98**, 4563–4568. doi:10.1073/pnas.081068098

Boland DJ, Brooker MIH, Chippendale GM, Hall N, Hyland BPM, Johnston RD, Kleinig DA, Turner JD (1985) 'Forest trees of Australia.' 4th edn. (Nelson and CSIRO: Melbourne)

Bowman DMJS (1997) Observations on the demography of the Australian boab (*Adansonia gibbosa*) in the north-west of the Northern Territory, Australia. *Australian Journal of Botany* **45**, 893–904. doi:10.1071/BT96092

Bowman DMJS, Brown GK, Braby MF, Brown JR, Cook LG, Crisp MD, Ford F, Haberle P, Hughes J, Isagi Y, Joseph L, McBride J, Nelson G, Ladiges PY (2010) Biogeography of the Australian monsoon tropics. *Journal of Biogeography* **37**, 201–216. doi:10.1111/j.1365-2699.2009.02210.x

Brock J (1988) 'Top End native plants.' (Brock: Darwin)

Brummitt RK (2002) A consideration of 'Nomina Subnuda'. *Taxon* **51**, 171–174. doi:10.2307/1554976

Byrne M, Yeates DK, Joseph L, Kearney M, Bowler J, Williams MAJ, Cooper Donnellan SC, Keogh JS, Leys R, Melville J, Murphy DJ, Porch N, Wyrwoll K-H (2008) Birth of a biome: insights into the assembly and maintenance of the Australian arid zone biota. *Molecular Ecology* **17**, 4398–4417. doi:10.1111/j.1365-294X.2008.03899.x

Chen C, Durand E, Forbes F, François O (2007) Bayesian clustering algorithms ascertaining spatial population structure: a new computer program and comparison study. *Molecular Ecology Notes* **7**, 747–756. doi:10.1111/j.1471-8286.2007.01769.x

Clark PU, Dyke AS, Shakun JD, Carlson AE, Clark J, Wohlfarth B, Mitrovica JX, Hostetler SW, McCabe AM (2009) The Last Glacial Maximum. *Science* **325**, 710–714. doi:10.1126/science.1172873

Cornuet J-M, Luikart G (1996) Description and power analysis of two tests for detecting recent population bottlenecks from allele frequency data. *Genetics* **144**, 2001–2014.

Cunningham A (1827) Natural history appendix. In 'Narrative of a survey of the intertropical and western coasts of Australia performed between the years 1818 and 1822'. (Ed. PP King) pp. 408–629. (John Murray: London)

Duvall CS (2007) Human settlement and baobab distribution in south-western Mali. *Journal of Biogeography* **34**, 1947–1961. doi:10.1111/j.1365-2699.2007.01751.x

Earl DA, von Holdt BM (2012) STRUCTURE HARVESTER: a website and program for visualizing STRUCTURE output and implementing the Evanno method. *Conservation Genetics Resources* **4**, 359–361. doi:10.1007/s12686-011-9548-7

Eldridge MDB, Potter S, Cooper SJB (2011) Biogeographic barriers in north-western Australia: an overview and standardisation of nomenclature. *Australian Journal of Zoology* **59**, 270–272. doi:10.1071/ZO12012

Estoup A, Jarne P, Cornuet J-M (2002) Homoplasy and mutation model at microsatellite loci and their consequences for population genetics analysis. *Molecular Ecology* **11**, 1591–1604. doi:10.1046/j.1365-294X.2002.01576.x

Evanno G, Regnaut S, Goudet J (2005) Detecting the number of clusters of individuals using the software STRUCTURE: a simulation study. *Molecular Ecology* **14**, 2611–2620. doi:10.1111/j.1365-294X.2005.02553.x

Excoffier L, Smouse PE, Quattro JM (1992) Analysis of molecular variance inferred from metric distances among DNA haplotypes: application to human mitochondrial DNA restriction data. *Genetics* **131**, 479–491.

Falush D, Stephens M, Pritchard JK (2003) Inference of population structure using multilocus genotype data: linked loci and correlated allele frequencies. *Genetics* **164**, 1567–1587.

François O, Ancelet S, Guillot G (2006) Bayesian clustering using hidden Markov random fields in spatial population genetics. *Genetics* **174**, 805–816. doi:10.1534/genetics.106.059923

Gillison AN (1983) Tropical savannas of Australia and southwest Pacific. In 'Tropical savannas. Vol. 13'. (Ed. F Bourliere) pp. 183–243. (Elsevier Scientific Publishing: Amsterdam)

Hey J, Nielsen R (2004) Multilocus methods for estimating population sizes, migration rates and divergence time, with applications to the divergence of *Drosophila pseudoobscura* and *D. persimilis*. *Genetics* **167**, 747–760. doi:10.1534/genetics.103.024182

Hill KD, Johnson LAS (1995) Systematic studies in the eucalypts. 7. A revision of the bloodwoods, genus *Corymbia* (Myrtaceae). *Telopea* **6**, 185–504.

Jakobsson M, Rosenberg NA (2007) CLUMPP: a cluster matching and permutation program for dealing with label switching and multimodality in analysis of population structure. *Bioinformatics* **23**, 1801–1806. doi:10.1093/bioinformatics/btm233

James EA, Brown GK, Citroen R, Rossetto M, Porter C (2011) Development of microsatellite loci in *Triglochin procera* (Juncaginaceae), a polyploid wetland plant. *Conservation Genetics Resources* **3**, 103–105. doi:10.1007/s12686-010-9301-7

Jombart T, Devillard S, Dufour A-B, Pontier D (2008) Revealing cryptic spatial patterns in genetic variability by a new multivariate method. *Heredity* **101**, 92–103. doi:10.1038/hdy.2008.34

Kershaw P (1995) Environmental change in Greater Australia. *Antiquity* **69**, 656–675.

Larsen AS, Vaillant A, Verhaegen D, Kjær ED (2009) Eighteen SSR-primers for tetraploid *Adansonia digitata* and its relatives. *Conservation Genetics Resources* **1**, 325–328. doi:10.1007/s12686-009-9075-y

Lowe P (1998) 'The boab tree.' (Lothian Books: Melbourne)

Luikart G, Allendorf F, Cornuet J-M, Sherwin W (1998) Distortion of allele frequency distributions provides a test for recent population bottlenecks. *The Journal of Heredity* **89**, 238–247. doi:10.1093/jhered/89.3.238

McConnell K, O'Connor S (1997) 40,000 year record of food plants in the Southern Kimberley Ranges, Western Australia. *Australian Archaeology* **45**, 20–31.

McConnell K, O'Connor S (1999) Carpenter's Gap shelter I: a case for total recovery. In 'Taphonomy: the analysis of processes from phytoliths to megafauna'. (Eds MJ Mountain, D Bowdery) pp. 23–34. (ANH Publications: Canberra)

Melville J, Ritchie EG, Chapple SNJ, Glor RE, Schulte JA (2011) Evolutionary origins and diversification of dragon lizards in Australia's tropical savannas. *Molecular Phylogenetics and Evolution* **58**, 257–270. doi:10.1016/j.ympev.2010.11.025

Meirmans PG (2012) The trouble with isolation by distance. *Molecular Ecology* **21**, 2839–2846. doi:10.1111/j.1365-294X.2012.05578.x

Mueller F von (1857) New genera and species. *Hooker's journal of botany and Kew Garden miscellany* **9**, 14.

Mueller F von (1858) Botanical report on the North Australian exploring expedition. *Proceedings of the Linnean Society of London (Botany)* **2**, 140–149.

Mueller F von (1893) Botanical notes from north-west Australia. *Victorian Naturalist* **10**, 110–111.

Oliver PM, Adams M, Doughty P (2010) Molecular evidence for ten species and Oligo–Miocene vicariance within a nominal Australian gecko species (*Crenadactylus ocellatus*, Diplodactylidae). *BMC Evolutionary Biology* **10**, 386. doi:10.1186/1471-2148-10-386

Peakall R, Smouse PE (2006) GENALEX 6: genetic analysis in Excel. Population genetic software for teaching and research. *Molecular Ecology Notes* **6**, 288–295. doi:10.1111/j.1471-8286.2005.01155.x

Pettigrew J (2011) Iconography in Bradshaw rock art: breaking the circularity. *Clinical & Experimental Optometry* **94**, 403–417. doi:10.1111/j.1444-0938.2011.00648.x

Pettigrew JD, Bell KL, Bhagwandin A, Grinan E, Jillani N, Meyer J, Wabuyele E, Vickers CE (2012) Morphology, ploidy and molecular phylogenetics reveal a new diploid species from Africa in the baobab genus *Adansonia* (Bombacoideae; Malvaceae). *Taxon* **61**, 1240–1250.

Potter S, Eldridge MDB, Cooper SJB, Paplinska JZ, Taggart DA (2012*a*) Habitat connectivity, more than species' biology, influences genetic differentiation in a habitat specialist, the short-eared rock-wallaby (*Petrogale brachyotis*). *Conservation Genetics* **13**, 937–952. doi:10.1007/s10592-012-0342-1

Potter S, Eldridge MDB, Taggart DA, Cooper SJB (2012*b*) Multiple biogeographical barriers identified across the monsoon tropics of northern Australia: phylogeographic analysis of the *brachyotis* group of rock-wallabies. *Molecular Ecology* **21**, 2254–2269. doi:10.1111/j.1365-294X.2012.05523.x

Pritchard JK, Stephens M, Donnelly P (2000) Inference of population structure using multilocus genotype data. *Genetics* **155**, 945–959.

R Development Core Team (2008) 'R: a language and environment for statistical computing.' (R foundation for Statistical Computing: Vienna)

Raven PH, Axelrod DI (1974) Angiosperm biogeography and past continental movements. *Annals of the Missouri Botanical Garden* **61**, 539–673. doi:10.2307/2395021

Rosenberg NA (2004) DISTRUCT: a program for the graphical display of population structure. *Molecular Ecology Notes* **4**, 137–138. doi:10.1046/j.1471-8286.2003.00566.x

Shaw J, Lickey EB, Schilling EE, Small RL (2007) Comparison of whole chloroplast genome sequences to choose noncoding regions for phylogenetic studies in angiosperms: the tortoise and the hare III. *American Journal of Botany* **94**, 275–288. doi:10.3732/ajb.94.3.275

Sun JX, Mullikin JC, Patterson N, Reich DE (2009) Microsatellites are molecular clocks that support accurate inferences about history. *Molecular Biology and Evolution* **26**, 1017–1027. doi:10.1093/molbev/msp025

Thuillet A-C, Bru D, David J, Roumet P, Santoni S, Sourdille P, Bataillon T (2002) Direct estimation of mutation rate for 10 microsatellite loci in durum wheat, *Triticum turgidum* (L.) Thell. ssp. *durum* desf. *Molecular Biology and Evolution* **19**, 122–125. doi:10.1093/oxfordjournals.molbev.a003977

Wallis LA (2001) Environmental history of northwest Australia based on phytolith analysis at Carpenter's Gap 1. *Quaternary International* **83–85**, 103–117. doi:10.1016/S1040-6182(01)00033-7

Wickens GE (1982) The baobab: Africa's upside-down tree. *Kew Bulletin* **37**, 173–209. doi:10.2307/4109961

Wickens GE, Lowe P (2008) 'The baobabs: pachycauls of Africa, Madagascar, and Australia.' (Springer: Berlin)